EurJOC

European Journal of Organic Chemistry

Chemistry Europe

European Chemical Societies Publishing

Accepted Article

Title: Substrate Photoswitching for Rate Enhancement of an Organocatalytic Cyclization Reaction

Authors: Matej Zabka and Ruth M. Gschwind

To be cited as: *Eur. J. Org. Chem.* **2022**, e202200048

Link to VoR: https://doi.org/10.1002/ejoc.202200048

WILEY-VCH

WILEY-VCH

RESEARCH ARTICLE

Substrate Photoswitching for Rate Enhancement of an Organocatalytic Cyclization Reaction

Matej Žabka and Ruth M. Gschwind*[a]

Abstract: In this article, we report that applying *in situ* LED-NMR irradiation with appropriate wavelength resulted in the photoswitching of an α,β-unsaturated hydrazone C=N double bond configuration. This reaction was previously reported to be the first step in a chiral Brønsted acid-catalyzed cyclization reaction, where the minor but stable *Z*-isomer is the reactive intermediate. By enhancing the rate of the isomerization, we could show that the overall rate of the cyclization could be increased and followed directly by NMR kinetics. Exclusively light with a specific wavelength matching the isomerization process affected the cyclization. The light- and acid-mediated isomerization provide complementary pathways that can be exploited in synthetic applications to increase reaction rates of asymmetric transformations, especially in reactions requiring high loadings of elaborate chiral catalysts.

Introduction

Absorption of visible light by a substrate, intermediate or catalyst in catalytic reactions can enable new reactivities,[1,2] promote alternative pathways, and modify reaction rates[3] or selectivity.[4] A powerful method to monitor and evaluate these changes is NMR spectroscopy, which also provides detailed quantitative and structural information at the same time. The most cost-effective and straightforward combination of these two approaches – the LED-NMR setup – enables light-emitting diode (LED) illumination inside the NMR.[5–7] This method, developed mainly in our research group, proved valuable in mechanistic studies of many photocatalytic and organocatalytic reactions,[6–8] as well as photoisomerizations.[9–11] In the context of asymmetric catalysis, switching of C=C or C=N double bonds in catalysts, substrates or intermediates can alter the reaction outcome in terms of chemical yield or selectivity as long as the *E*- and *Z*-isomers have distinct reactivities or lead to a different stereoisomer of the product. So far, this has been shown predominantly with photoswitchable catalysts,[12] enamines,[13] as well as with imines and substituted alkenes as typical substrates.[14–19] While imines can be isomerized directly by visible light irradiation (350 – 400 nm),[20] substituted alkenes require the use of a photosensitizer.[15–19,21–23] The *E*/*Z* selectivity is due to subtle differences in chromophore conjugation, triplet energies, and the different efficiency of energy transfer to *E*- and *Z*-isomers,[22] which requires specifically designed substitution patterns that could limit the broad scope.

[a] Dr. M. Žabka, Prof. Dr. R. M. Gschwind
Institute of Organic Chemistry
Universität Regensburg
Universitätstrasse 31, 93053 Regensburg
E-mail: ruth.gschwind@chemie.uni-regensburg.de
Webpage: http://www-oc.chemie.uni-regensburg.de/gschwind/index.html

Supporting information for this article is given via a link at the end of the document.

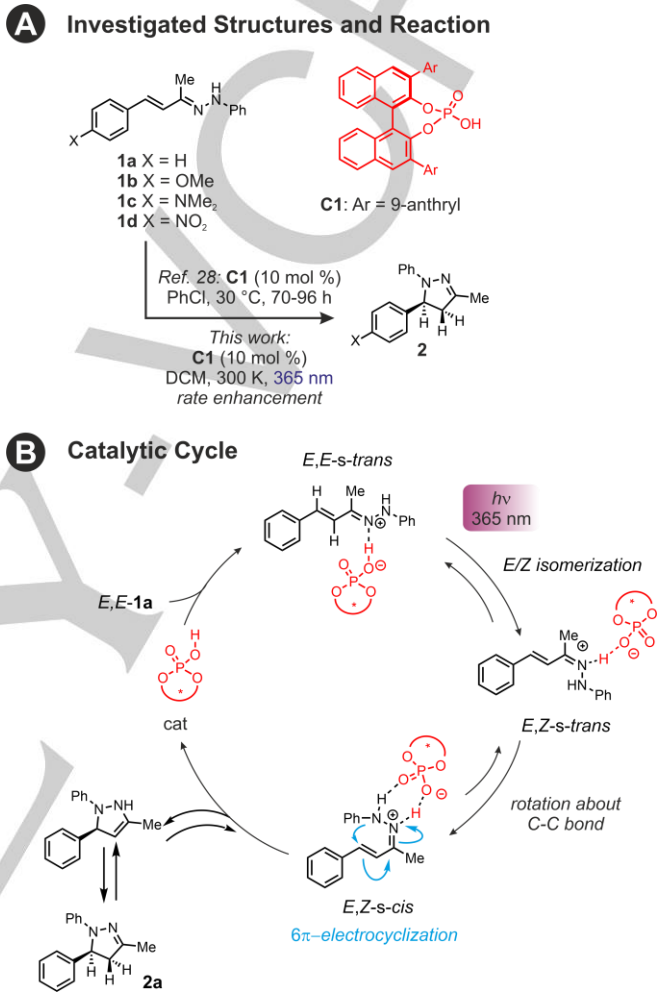

Scheme 1. a) Structures of the investigated compounds and the investigated reaction. b) Catalytic cycle for the CPA-catalyzed electrocyclization is shown starting from *E,E*-**1a**. The formation of *E,Z*-isomer and rotation about C-C bond are required for the reaction to give the cyclized product **2a**.

However, in many (photo)switchable devices, visible-light absorbing acylhydrazones are used extensively.[24–26] Hydrazones are also widely explored substrates in organocatalysis and thus attractive for mechanistic investigations.[27] Therefore, we sought to exploit a potential photoisomerization process inside a catalytic cycle involving simple conjugated hydrazones (for the structures see Scheme 1A) without any sensitizer. A chiral phosphoric acid (CPA)-catalyzed 6π electrocyclization of α,β-unsaturated hydrazones that provides 2-pyrazolines, reported by List et al.,[28,29] is a suitable reaction to test this idea (Scheme 1A). The reaction was studied by computational methods and was classified as "pseudopericyclic ring closure involving an intramolecular nucleophilic addition".[30] Indeed, for the ring closure, the *E,Z*-s-*cis* conformation is required for the reaction to proceed and must be formed from the most stable ***E,E***-s-*trans* conformation (Scheme 1B).

Results and Discussion

Photoisomerization of hydrazones

To verify the photoswitching of the substrate and *E/Z* isomerization of the C=N bond, pure hydrazone *E,E*-**1a** (initial C=N *E/Z* ratio 99.5:0.5, Figure 1A) was subjected to LED irradiation of 365 nm in CD_2Cl_2 at 300 K. Indeed, the major *E,E*-isomer was converted into the *E,Z*-hydrazone (25:75 C=N *E/Z* ratio at photostationary state, see Figure 1A). The C=C double bond was untouched by the irradiation and remained *E*-configured (for details see SI Chapter 6.1). To our delight, the formed *E,Z*-isomer is relative stable and even after 75 minutes in the dark, its concentration decreases only slightly to around 70%. Interestingly, aryl substituents had a pronounced effect on the isomerization process. An electron-donating methoxy group at the aromatic ring in **1b** increased the isomerization rate but less *Z*-isomer was obtained in the photostationary state (~60 % *E,Z*, see Scheme 1A for structures and Table 1 for rates). An even larger isomerization rate for the *E,E*-isomer was observed with dimethylamino-derivative **1c**. However, with **1c** also the isomerization of the C=C bond took place and additional *Z,E*-isomer was formed. In contrast, strong electron-withdrawing group such as nitro (**1d**) prevented efficient photoisomerization. The correlation of the photoisomerization rate constants with Hammett σ_p constants is consistent with the assumption that the isomerization is the rate determining step in the cyclization reaction (see SI Chapter 5.1). Interestingly, we found a very good correlation between the reported achiral acid-promoted cyclization rates[31] and our photoisomerization rates (see SI Chapter 5.1), further corroborating this assumption.

Cyclization reaction

These results encouraged us to exploit photoisomerization of **1a** in the catalytic reaction with **C1** (10 mol %) (Figure 1B). After applying 365 nm irradiation, the product formation rate was increased by a factor of 2.35 solely due to the substrate photoswitching with the light wavelength corresponding to the absorption maximum of **1a** (Figure 1B). A similar magnitude of rate enhancement with 365 nm was observed with substrate **1b**. The enhanced rate is an improvement given the high catalyst loading and slow “dark” reaction rate. Other investigated wavelengths did not have any impact on the reaction rate. Overall, we have shown that applying light irradiation can increase the rate of a catalytic reaction. The *ee* of the products **2a**, **2b** and **2d** should not be affected by the photoisomerization since a selective photoisomerization of the C=N double bond is achieved. However, this premise could not be confirmed as we were not able to determine the enantiomeric excess (for further details see SI Chapter 4.3).

Next, we studied the binary complex of CPA and hydrazone by NMR at low temperature. Previously, we were able to obtain structural information about CPA and DSI binary and ternary complexes with imines.[32–34] Thus, we prepared a CPA **C1**/(*E*)-**1a** 1:1 complex in CD_2Cl_2 and acquired NMR spectra at 233 K. At this temperature, acid-promoted isomerization is stopped. Two distinct hydrogen bond signals emerged in a 1:1 ratio (δ_H 12.87 and 9.60 ppm), corresponding to the two NH sites of the protonated hydrazone. Two well separated ^{31}P peaks (1:1 ratio) clearly show the existence of two complexes in slow exchange on the phosphorous NMR time scale (on the proton NMR time scale these complexes are in fast exchange). The $^{1}H,^{31}P$-HMBC allylic-type correlations show clearly that in one complex the phosphoric acid is bound to the iminium type nitrogen and in the other complex to the amine type nitrogen. A bifunctional binding as expected[28] is definitely not present in the *E,E*-configured complexes investigated (for the structures and details see SI Chapter 7.2).

In situ 365 nm light irradiation of **C1**/**1a** at low temperature did not isomerize the intermediate chiral acid/*E*-hydrazonium complex, probably due to shifted absorption maximum of the protonated species. Thus, any light-induced isomerization must occur outside of the H-bonded complex at reaction conditions.

Additionally, the sample concentration had a profound effect on the photoisomerization rate at 300 K. Increasing the concentration of **1a** from 25 to 50 mM doubled the rate, but further increase to 100 mM led to a dramatic decrease in the reaction rate. This could hint at the quenching of the excited state with the ground state molecules in concentrated samples. Electron donors, such as amines, and presumably hydrazones, can quench both singlet and triplet excited states.[35]

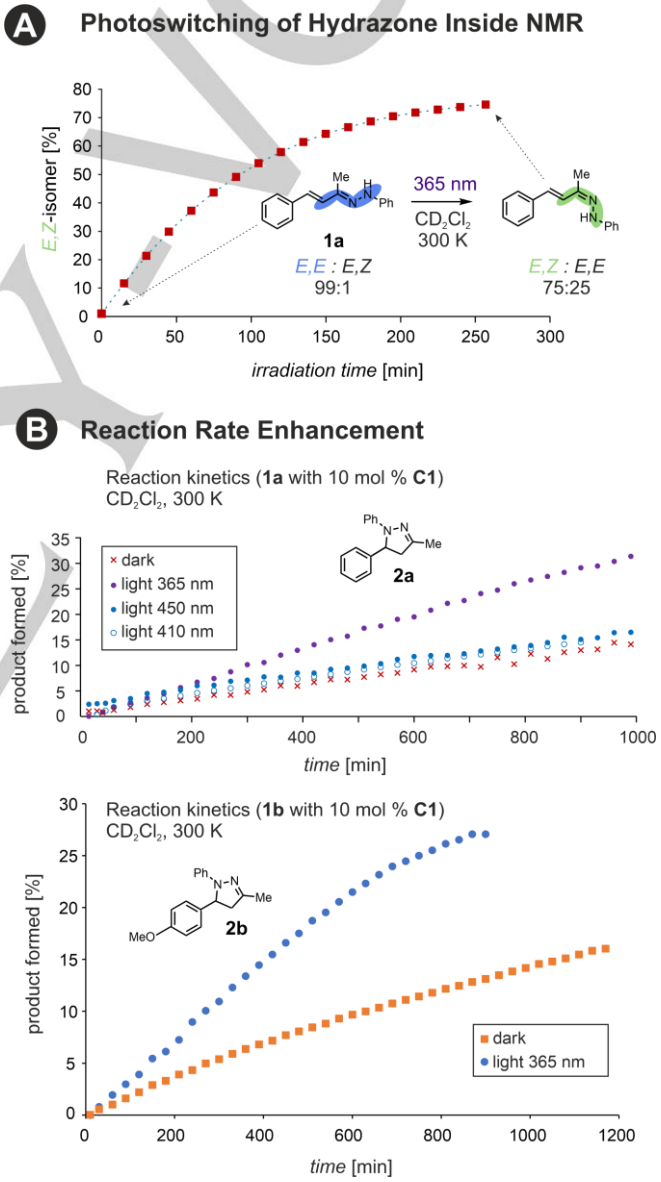

Figure 1. a) Photoswitching of *E,E*-**1a** with LED-NMR resulted in the formation of a stable *E,Z*-isomer. b) Reaction rate for the formation of **2a** and **2b** was enhanced with 365 nm light irradiation corresponding to the *E/Z*-isomerization process, but not by other wavelengths.

10.1002/ejoc.202200048

RESEARCH ARTICLE

A computational study of the isomerization was conducted at the DFT level of theory (Figure 2A). Vertical excitations ($S_0 \rightarrow S_1$) of 328 and 293 kJ·mol^{-1} (absorption of 365 and 408 nm light) were calculated for the *E,E*- and *E,Z*-**1a**, respectively, corresponding to HOMO-LUMO transition composed of π,π* and n,π*-orbitals (Figure 2A). The ground state *E,Z*-isomer is +9.20 kJ·mol^{-1} less stable (ΔG_{298}) than the *E,E*-isomer (for the complete energetical diagram including singlet and triplet states, see SI Chapter 8.5). Upon reaching the S_1 state from ground S_0 state for both *E*- and *Z*-hydrazones, the double-bond character of C=N is reduced enabling an isomerization by rotation, as evidenced by lengthening of the C=N bond (1.297 Å → 1.353 Å) and shortening of the single =C-C bond, as well as a large change in C=N-N-C_{Ar} dihedral angle (see Figure 2A and SI Table 12). We explored the possibility of accessing the triplet state, in which the C-N bond could rotate, however, the exact mechanism for isomerization is not clear and two possibilities (torsional rotation and inversion) are proposed in the literature for imines and azobenzenes.[36,37] Interestingly, the computed structure of protonated *E,E*-**1a** also shows the dihedral angle twist and bond lengths similar to S_1 state and suggests a similar route in both acid- and light-promoted isomerization. Furthermore, TD-DFT calculations[38] (using PBE0/def2-TZVP/SMD(CH_2Cl_2)[39] or CAM-B3LYP for **1d** with charge-transfer character,[40] based on B3LYP-D3(BJ)/def2-TZVP geometries) provided a good match with the experimental UV-VIS spectra for hydrazones **1a** – **1d**. Similar results were obtained using higher level DLPNO-STEOM-CCSD/def2-TZVPP method (see SI Chapter 8.8).[41] The additional results for derivatives **1b** – **1d** are summarized in Table 1. Experimental values shift to higher wavelengths with both electron-donating and withdrawing substituents due to the extended conjugated donor-acceptor system. Overall, a good match of absorption maxima was obtained using both TD-DFT and STEOM calculations (see Figure 2B). These results show that designing rigid substrates with desired absorption properties by computational methods is possible.

Table 1. Photoisomerization rate constants (CD_2Cl_2, 300 K, 365 nm); isomer ratio at photostationary state (PSS); as well as experimental and calculated UV-VIS absorption maxima [nm] corresponding to *n*,π*/π,π*-transitions;.

Compound	Isomerization rate constants [min^{-1}]	*E,E* / *E,Z* / *Z,X* ratio at PSS (365 nm)	Exp. λ_{max}[a]	TD-DFT[b]	STEOM[c]
E,E-**1a**	0.010	25:75:0	351	365.2	340.5
E,Z-**1a**			-	408.1	364.7
E,E-**1b**	0.019	40:60:0	352	352.1	337.9
E,E-**1c**	0.026[d]	10:55:34	371	365.7	364.5
E,E-**1d**	0.002	92:8:0[e]	419	441.7[f]	437.8

[a] in CH_2Cl_2 at 25°C. [b] PBE0 functional. [c] DLPNO-STEOM-CCSD [d] Based on the decrease of *E,E*-**1c** [e] No isomerization occured with 450 nm light. [f] CAM-B3LYP functional.

Conclusion

LED-NMR approach is a fast and straightforward approach to tackle mechanistic observations in photo- and organocatalysis. Here, we exploited this technique to gain further insights about a catalytic cyclization reaction of hydrazones.

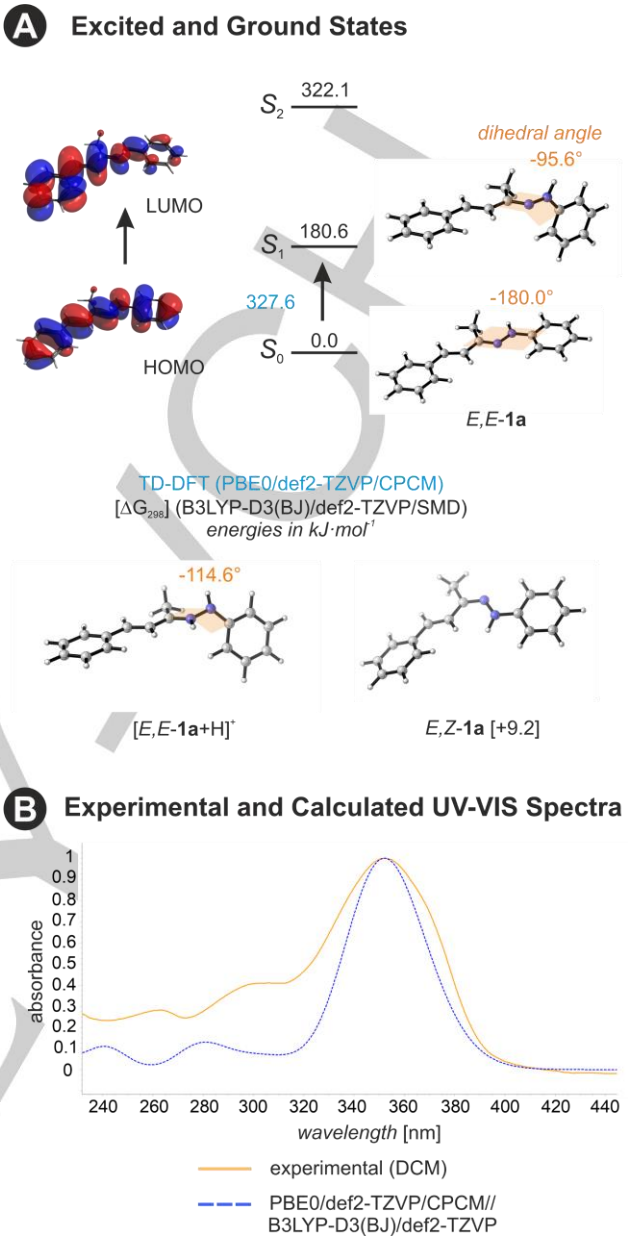

Figure 2. a) HOMO and LUMO orbitals of *E,E*-1a corresponding to the lowest energy transition involving n,π* and π,π*-orbitals of C=C-C=N (left); energetic diagram of ground and excited singlet states of 1a with calculated ΔG_{298} and TD-DFT vertical excitation energy. The geometries of the first excited state and protonated ground state are similar, suggesting similar pathways in the acid- and light-promoted isomerization. Computed structure of *E,Z*-1a is also shown. For more details, see SI Chapter 8.7. b) Match of experimental (solid orange line) and computed, unshifted (PBE0/def2-TZVP/CPCM – blue dashed line) UV-VIS spectra of *E,E*-1b.

We proved that light irradiation resulting exclusively in substrate photoswitching can enhance reactivity for slow reactions. This process is complementary to the acid-promoted isomerization in the case of cyclization of unsaturated hydrazones and can be used as an additional and/or alternative promoter of reactivity. Additional low temperature NMR experiments provided evidence for two monofunctional complexes, but did not prove the bifunctional binding of an *E,E*-hydrazone to the chiral phosphoric acid as previously proposed. As hydrazones are interesting for their reactivity and use in

photoswitchable devices, we also provided computational results that can explain their absorption and photoswitching abilities. We hope these results will encourage researchers to apply the presented methods to investigate other catalytic systems.

Experimental Section

Experimental Procedures: An amber-glass NMR tube was charged with hydrazone **1a** (5.90 mg, 0.025 mmol). The tube was evacuated under vacuum and backfilled with argon (3 x). Freshly distilled CD_2Cl_2 (0.5 mL) was added to reach the required concentration (50 mM). Optical fibre was inserted into the tube, sealed with parafilm, and the fibre connected to a 365 nm light-emitting diode (LED). The sample was inserted into Bruker AVANCE 600 MHz spectrometer equipped with TBI-F probe, tempered to 300 K, locked and shimmed. The light was switched on, the NMR kinetics measurement started and a standard ^{1}H NMR spectrum (NS 16, AQ 4.54 s, TD 64K, D1 2s) was acquired every 15 min.

Catalytic cycle investigations: A Schlenk flask was charged with **C1** (8.75 mg, 0.0125 mmol) and heated under vacuum at 150 °C for 15 min. After cooling down, the tube was flushed with argon. 1,3,5-trimethoxybenzene (2.10 mg, 0.0125 mmol) was added as NMR standard, followed by freshly distilled CD_2Cl_2 (2.5 mL). The solution was cooled down to -80°C in EtOAc/N_2(l) bath. An amber-glass NMR tube was charged with hydrazone **1a** (5.90 mg, 0.025 mmol). The tube was evacuated under vacuum and backfilled with argon (3 x). An aliquot of the **C1** solution (0.5 mL, 0.0025 mmol, 10 mol %; containing 0.1 eq. of the standard) was then added at -80°C to prevent the reaction from starting. Optical fibre was inserted into the tube, sealed with parafilm, with the other end connected to a 365 nm light-emitting diode (LED). The sample was inserted into Bruker AVANCE 600 MHz spectrometer equipped with TBI-F probe, tempered to 300 K. The light was switched on, the NMR kinetics measurement started and standard ^{1}H NMR spectra acquired. For the control dark reaction, the optical fibre was inserted into the NMR tube, but light was switched off during the experiment.

Computational Details: All computations were done in in ORCA 4.1.1 computational software.[42] Geometries were optimized at B3LYP-D3(BJ)/def2-TZVP level of theory. Geometries of the excited states (singlets and triplets) were optimized using TD-B3LYP-D3(BJ)/def2-TZVP level of theory. Numerical vibrational frequency calculations using the qRRHO method by Grimme were performed at the same level to confirm the stationary points as minima.[43] SMD solvation and Gibbs energy correction at 298 K were added to obtain ΔG_{298}. TD-DFT calculations with Tamm-Dancoff approximation were performed with PBE0 or CAM-B3LYP hybrid density functionals using def2-TZVP basis set and CPCM(dichloromethane) solvation model. Typically, 25 roots were requested.

Acknowledgements

This project was funded by the DFG (GS 13/4-2 project number 245388561 and RTG 2620/1 project number 426795949). We thank Denis Schekin for assistance with some experiments.

Keywords: Hydrazones • NMR spectroscopy • Organocatalysis • Photoswitching • Reaction mechanism

[1] M. Silvi, P. Melchiorre, *Nature* **2018**, *554*, 41–49.
[2] D. Staveness, J. L. Collins, R. C. McAtee, C. R. J. Stephenson, *Angew. Chem. Int. Ed.* **2019**, *58*, 19000–19006.
[3] P. Renzi, J. Hioe, R. M. Gschwind, *Acc. Chem. Res.* **2017**, *50*, 2936–2948.
[4] D. Niedek, F. R. Erb, C. Topp, A. Seitz, R. C. Wende, A. K. Eckhardt, J. Kind, D. Herold, C. M. Thiele, P. R. Schreiner, *J. Org. Chem.* **2020**, *85*, 1835–1846.
[5] C. Feldmeier, H. Bartling, E. Riedle, R. M. Gschwind, *J. Magn. Reson.* **2013**, *232*, 39–44.
[6] Y. Ji, D. A. DiRocco, J. Kind, C. M. Thiele, R. M. Gschwind, M. Reibarkh, *ChemPhotoChem* **2019**, *3*, 984–992.
[7] P. Nitschke, N. Lokesh, R. M. Gschwind, *Prog. Nucl. Magn. Reson. Spectrosc.* **2019**, *114–115*, 86–134.
[8] K. L. Skubi, W. B. Swords, H. Hofstetter, T. P. Yoon, *ChemPhotoChem* **2020**, *4*, 685–690.
[9] C. Wolff, J. Kind, H. Schenderlein, H. Bartling, C. Feldmeier, R. M. Gschwind, M. Biesalski, C. M. Thiele, *Magn. Reson. Chem.* **2016**, *54*, 485–491.
[10] J. Kind, L. Kaltschnee, M. Leyendecker, C. M. Thiele, *Chem. Commun.* **2016**, *52*, 12506–12509.
[11] M. W. H. Hoorens, M. Medved', A. D. Laurent, M. Di Donato, S. Fanetti, L. Slappendel, M. Hilbers, B. L. Feringa, W. Jan Buma, W. Szymanski, *Nat. Commun.* **2019**, *10*, 1–11.
[12] R. Dorel, B. L. Feringa, *Chem. Commun.* **2019**, *55*, 6477–6486.
[13] M. Huang, L. Zhang, T. Pan, S. Luo, *Science* **2022**, *375*, 869–874.
[14] P. Renzi, J. Hioe, R. M. Gschwind, *J. Am. Chem. Soc.* **2017**, *139*, 6752–6760.
[15] J. J. Molloy, J. B. Metternich, C. G. Daniliuc, A. J. B. Watson, R. Gilmour, *Angew. Chem. Int. Ed.* **2018**, *57*, 3168–3172.
[16] T. Hostmann, J. J. Molloy, K. Bussmann, R. Gilmour, *Org. Lett.* **2019**, *21*, 10164–10168.
[17] S. I. Faßbender, J. J. Molloy, C. Mück-Lichtenfeld, R. Gilmour, *Angew. Chem. Int. Ed.* **2019**, *58*, 18619–18626.
[18] J. J. Molloy, T. Morack, R. Gilmour, *Angew. Chem. Int. Ed.* **2019**, *58*, 13654–13664.
[19] K. Livingstone, M. Tenberge, F. Pape, C. G. Daniliuc, C. Jamieson, R. Gilmour, *Org. Lett.* **2019**, *21*, 9677–9680.
[20] J. M. Lehn, *Chem. – Eur. J.* **2006**, *12*, 5910–5915.
[21] T. Hostmann, T. Neveselý, R. Gilmour, *Chem. Sci.* **2021**, *12*, 10643–10648.
[22] T. Neveselý, M. Wienhold, J. J. Molloy, R. Gilmour, *Chem. Rev.* **2022**, *122*, 2650–2694.
[23] J. J. Molloy, M. Schäfer, M. Wienhold, T. Morack, C. G. Daniliuc, R. Gilmour, *Science* **2020**, *369*, 302–306.
[24] S. M. Landge, E. Tkatchouk, D. Benítez, D. A. Lanfranchi, M. Elhabiri, W. A. Goddard, I. Aprahamian, *J. Am. Chem. Soc.* **2011**, *133*, 9812–9823.
[25] I. Aprahamian, *Chem. Commun.* **2017**, *53*, 6674–6684.
[26] I. Cvrtila, H. Fanlo-Virgós, G. Schaeffer, G. Monreal Santiago, S. Otto, *J. Am. Chem. Soc.* **2017**, *139*, 12459–12465.
[27] M. de Gracia Retamosa, E. Matador, D. Monge, J. M. Lassaletta, R. Fernández, *Chem. – Eur. J.* **2016**, *22*, 13430–13445.
[28] S. Müller, B. List, *Angew. Chem. Int. Ed.* **2009**, *48*, 9975–9978.
[29] S. Müller, B. List, *Synthesis* **2010**, 2171–2178.
[30] B. Heggen, M. Patil, W. Thiel, *J. Comput. Chem.* **2016**, *37*, 280–285.
[31] H. Ferres, M. S. Hamdam, W. R. Jackson, *J. Chem. Soc. B* **1971**, 1892–1898.
[32] J. Greindl, J. Hioe, N. Sorgenfrei, F. Morana, R. M. Gschwind, *J. Am. Chem. Soc.* **2016**, *138*, 15965–15971.
[33] K. Rothermel, M. Žabka, J. Hioe, R. M. Gschwind, *J. Org. Chem.* **2019**, *84*, 13221–13231.
[34] M. Žabka, R. M. Gschwind, *Chem. Sci.* **2021**, *12*, 15263–15272.
[35] G. Porcal, S. G. Bertolotti, C. M. Previtali, M. V. Encinas, *Phys. Chem. Chem. Phys.* **2003**, *5*, 4123–4128.
[36] S. K. Kandappa, L. K. Valloli, S. Ahuja, J. Parthiban, J. Sivaguru, *Chem. Soc. Rev.* **2021**, *50*, 1617–1641.
[37] E. Merino, M. Ribagorda, *Beilstein J. Org. Chem.* **2012**, *8*, 1071–1090.
[38] C. Adamo, D. Jacquemin, *Chem. Soc. Rev.* **2013**, *42*, 845–856.
[39] C. Adamo, V. Barone, *J. Chem. Phys.* **1999**, *110*, 6158–6170.

[40] T. Yanai, D. P. Tew, N. C. Handy, *Chem. Phys. Lett.* **2004**, *393*, 51–57.
[41] R. Berraud-Pache, F. Neese, G. Bistoni, R. Izsák, *J. Chem. Theory Comput.* **2020**, *16*, 564–575.
[42] F. Neese, F. Wennmohs, U. Becker, C. Riplinger, *J. Chem. Phys.* **2020**, *152*, 224108.
[43] S. Grimme, *Chem. – Eur. J.* **2012**, *18*, 9955–9964.

WILEY-VCH

RESEARCH ARTICLE

Entry for the Table of Contents

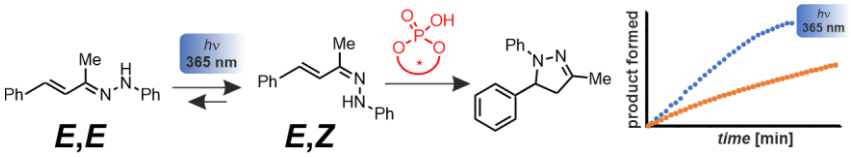

In organocatalysis, many transformations require quite high catalyst loadings, as the processes are sluggish and complex equilibria are involved. Here, we applied in situ light irradiation with specific wavelength inside NMR to increase reaction rates of hydrazone cyclization. This enhancement was achieved by isomerizing the substrate to the reactive configuration.